Fuel 216 (2018) 579–588

Contents lists available at ScienceDirect

Fuel

journal homepage: www.elsevier.com/locate/fuel

Impact of increasing methyl branches in aromatic hydrocarbons on diesel engine combustion and emissions

Midhat Talibi*, Paul Hellier, Nicos Ladommatos

Department of Mechanical Engineering, University College London, Torrington Place, London WC1E 7JE, United Kingdom

ARTICLE INFO

Keywords:
Diesel
Combustion
Engine
Toluene
Alkylbenzene
M-xylene

ABSTRACT

Lignocellulosic materials have been identified as potential carbon–neutral sources of sustainable power production. Catalytic conversion of lignocellulosic biomass results in liquid fuels with a variety of aromatic molecules. This paper investigates the combustion characteristics and exhaust emissions of a series of alkylbenzenes, of varying number of methyl branches on the monocyclic aromatic ring, when combusted in a direct injection, single cylinder, compression-ignition engine. In addition, benzaldehyde (an aldehyde (-CHO) branch on the monocyclic ring) was also tested. All the molecules were blended with heptane in different proportions, up to 60% wt/wt. The tests were conducted at a constant engine speed of 1200 rpm, a fixed engine load 4 bar IMEP, and at two injection modes: constant start of fuel injection at 10 CAD BTDC, and varying fuel injection timing to maintain constant start of fuel combustion at TDC.

The results showed that the ignition delay period increased with increasing number of methyl branches on the ring, due to the rapid consumption of OH radicals by the alkylbenzenes for oxidation to stable benzyl radicals. Peak heat release rates, and concurrently NOx emissions, initially increased with increasing methyl branches, but subsequently both decreased as the bulk of heat release occurred further into the expansion stroke with significant thermal energy losses. With the exception of toluene, the number of particles in the engine exhaust increased as the number of methyl branches on the aromatic ring increased, attributable to the formation of thermally stable benzyl radicals.

1. Introduction

There is international consensus on the adverse changes in global climate arising from anthropogenic emissions of carbon (CO_2, CH_4, particulates) from fossil fuel source [1,2]. This concern has resulted in legislative targets in many countries for the use of renewable alternatives in road transport fuels [3–5]. However, there is growing unease regarding the use of fuels primarily derived from food crops. For example, ethanol from of sugar fermentation and fatty acid esters (biodiesel) from vegetable oils may not offer significant reductions in GHG emissions when considering the entirety of the fuel production lifecycle and the arising changes in land-use [6–8]. At the same time, there is growing public concern about the adverse health effects of engine exhaust pollutants such as NOx and PM, reflected in the increasingly strict vehicle emissions standards and plans to ban diesel vehicles from major cities [9,10]. Therefore, there is a need to develop future fuels from sustainable non-food crop sources, which also produce lower toxic pollutant emissions.

Current renewable fuels for both spark ignition and diesel engines, predominantly bioethanol and fatty acid methyl esters (biodiesel) respectively, are acyclic and do not contain aromatic or cyclic constituents commonly found in liquid fossil fuels. Cyclic molecules are considered to be desirable as fuels for spark ignition engines as they generally exhibit high knock resistance [11]. Additionally, the higher energy density of aromatic molecules, relative to oxygenated acyclic molecules typical of current biofuels, also encourages their utilisation in fuel blends for diesel engines. For example, toluene, which is a cyclic aromatic, has a heating value of 40.60 MJ/kg [12], while that of methyl oleate, a common component of current biodiesel, is lower at 37.42 MJ/kg [13].

An alternative to the manufacture of fuels from feedstocks which are also suitable for food production, is to derive these fuels from associated crop residue material [14,15]. Such materials, which might otherwise be considered a waste-stream, often consist primarily of lignocellulosic biomass, comprising of lignin, cellulose and hemi-cellulose. Catalytic reformation processes, such as Fisher Tropsch, require the cleaving of all carbon to carbon bonds present in the biomass through the input of additional energy [16], and can yield a range of aliphatic molecules.

* Corresponding author.
E-mail address: m.talibi@ucl.ac.uk (M. Talibi).

https://doi.org/10.1016/j.fuel.2017.12.045
Received 26 May 2017; Received in revised form 8 December 2017; Accepted 12 December 2017

Nomenclature

ATDC	after-top-dead-centre
BTDC	before-top-dead-centre
CAD	crank angle degree
CH_4	methane
CI	compression ignition
CO	carbon monoxide
CO_2	carbon dioxide
H_2	hydrogen
IMEP	indicated mean effective pressures
NO	nitric oxide
NO_x	nitrogen oxides
O_2	oxygen
OH	hydroxyl
PM	particulate mass
ppm	parts per million
rpm	revolutions per minute
SOC	start of combustion
SOI	start of injection
TDC	top -dead -centre
THC	total hydrocarbons
φ_{CH4}	methane-air equivalence ratio
φ_{H2}	hydrogen-air equivalence ratio

Alternatively, the large polymers that make up lignin, cellulose and hemi-cellulose can also be converted to monomer units through the selective cleaving of specific targeted carbon to carbon bonds and carbon to oxygen bonds, which can be relatively less energy intensive [16,17].

Thring et al. [18] reported the conversion of lignin, over a zeolite catalyst in a fixed bed reactor, to gaseous and liquid products at temperatures between 500 °C to 650 °C with total yields of between 50% wt/wt to 85% wt/wt. Of this, the liquid fraction comprised approximately 80% wt/wt aromatic molecules consisting of benzene, toluene and xylene. As reaction temperatures were increased, the proportion of xylene present in the liquid fraction decreased while that of benzene and toluene increased. More recently, Zhang et al. [19] produced a mixture of benzene, toluene and xylene from the catalytic pyrolysis of sawdust mixed with a zeolite catalyst at temperatures between 450 °C and 600 °C. Similar to the observations of Thring et al. [18], it was found that increasing temperatures resulted in a reduction in the presence of methyl branches on the aromatic molecules, reducing the proportion of xylene present with a concurrent increase in levels of both toluene and benzene. Yan et al. [20] explored the conversion of duckweed (an aquatic plant which doubles in mass through growth every 24 h) to a crude liquid bio-oil via hydrothermal liquefaction, which consisted mostly of alkyl benzenes (toluene and benzene) and alkyl naphthalenes.

While benzene exhibits a higher cetane number than toluene (14.3 versus ~ 0 [21]), it is the latter which as a primary reference fuel has been more frequently tested as a blend component in diesel engines. Hellier et al. [22] tested a range of binary mixtures of toluene and n-heptane in a direct injection compression ignition engine at toluene levels of up to 52.2% and found an increase in the duration of ignition delay with toluene level being the primary driver of NOx levels in the exhaust. The addition of further methyl branches to aromatic and cyclic molecules has not been widely considered in the context of compression ignition, however, Baumgardner et al. [23] investigated the effects of blending various phenols potentially derived from biomass at either 2% or 5% with a reference fossil diesel. It was found that the addition of a further methyl branch to p-cresol to form 2,4-dimethylphenol resulted in a later time of peak heat release rate at constant injection timing when blended at 2% with reference fossil diesel and increased PM10 emissions at 50% and 75% load conditions. In addition, several researchers have observed an increase in sooting tendency (or threshold sooting index) with the addition of methyl branches to an aromatic ring in studies including benzene, toluene and xylenes in both diffusion [24,25] and premixed flames [26].

The study presented here investigates the effect of varying the number of methyl branches on a monocyclic aromatic ring, on the combustion and emissions of a diesel engine. Each of the aromatic molecules investigated were mixed with n-heptane to form binary blends, with the results baselined against reference fossil diesel fuel. Each fuel was tested at two injection timing modes, constant start of fuel injection and constant start of combustion. In addition to the gaseous exhaust emissions, this paper also describes the number and size distribution of the particulate emissions in the exhaust arising from combustion of the binary fuel blends.

2. Experimental setup

All experiments in the current work were conducted on a direct injection, water cooled, single cylinder compression-ignition engine, described in [27], consisting of 2.0 L, 4-cylinder Ford Duratorq cylinder head (including valves, piston and connecting rod) mounted on a Ricardo Hydra crankcase - Table 1 lists the details of the engine geometry. The in-cylinder gas pressure was measured to a resolution of 0.2 CAD using a Kistler 6056A piezoelectric pressure transducer in conjunction with a Kistler 5018 charge amplifier. Various other operational pressures and temperatures were also monitored live and logged on PCs using National Instruments (NI) data acquisition systems. An in-house developed NI LabVIEW program evaluated the in-cylinder pressure data in real-time to determine net apparent heat release rates and the indicated mean effective pressure (IMEP). A Delphi DFI 1.3 six-hole, servo-hydraulic solenoid valve fuel injector was used to inject liquid fuel directly into the combustion chamber, with an EmTronix EC-GEN500 system used to control the injection pressure, injection timing and duration of injection. The intake air flow rate was measured using a Romet G65 positive displacement volumetric air flow meter. Fig. 1 shows the schematic of the single cylinder engine facility, including the high pressure fuel delivery system described in the following paragraphs.

A bespoke high pressure fuel system, based on previous designs by Schonborn et al. [28] and Hellier et al. [29], was used to deliver liquid fuels, such as the n-alkylbenzene/heptane blends used in this study, to the fuel injector. The fuel system consisted of a stainless steel vessel with capped ends and a free moving piston. As shown in Fig. 1, the fuel system utilised the conventional common rail diesel engine system to supply hydraulic pressure to the vessel on one side of the piston. The diesel fuel could be pressurised precisely using the Emtronix control system, and the free moving piston communicated this pressure to the test fuel and, therefore, the test fuel could be injected into the engine at

Table 1
Engine specifications.

Bore	86 mm
Stroke	86 mm
Swept volume	499.56 cm^3
Compression ratio (geometric)	18.3:1
Maximum in-cylinder pressure	150 bar
Piston design	Central ω – bowl in piston
Intake/Exhaust valves	2/2
Fuel injection pump	Delphi single-cam radial-piston pump
High pressure common rail	Delphi solenoid controlled, 1600 bar max.
Diesel fuel injector	Delphi DFI 1.3 6-hole solenoid valve
Electronic fuel injection system	1 μs duration control
Crank shaft encoder	1800 ppr, 0.2 CAD resolution

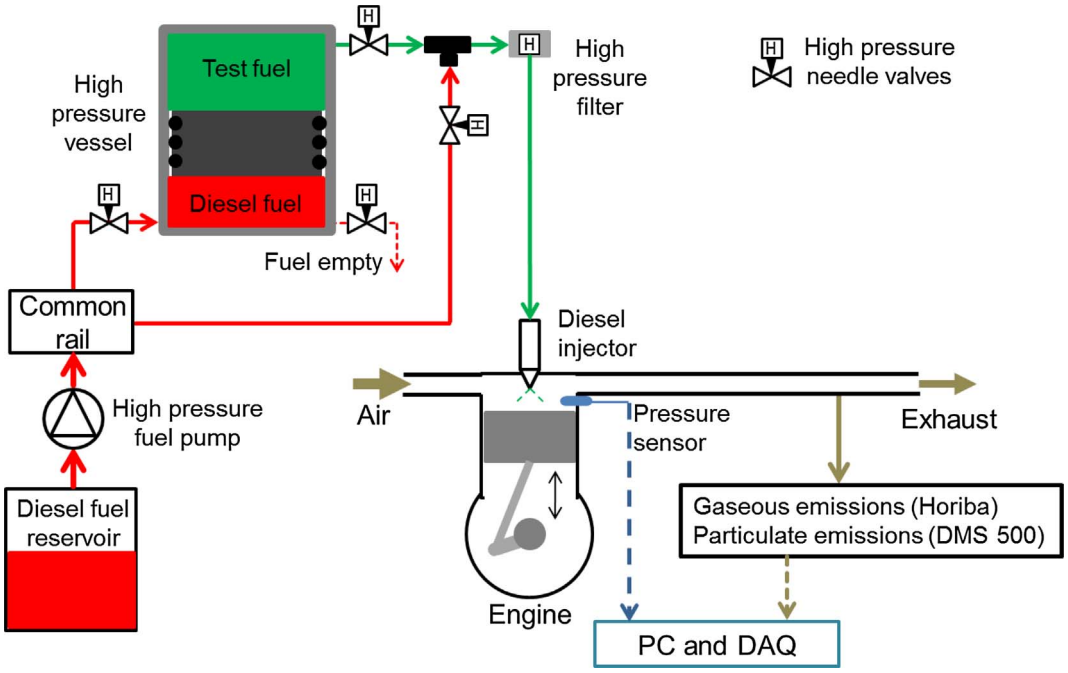

Fig. 1. Schematic showing test engine arrangement including the high pressure fuel delivery system and exhaust emissions instrumentation.

a selected common rail pressure. A filter was also installed between the vessel and the fuel injector to remove any debris in the test fuel which could damage the injector. The design and operation of the high pressure fuel system has been described in detail in [30].

The custom-made fuel system allowed the use of limited quantities of the test fuel blends (up to 1 L), as compared to the conventional diesel pump-common rail system which typically requires several litres of fuel and has a considerably higher risk of cross contamination when changing between different test fuel blends. Additionally, some of the test fuel blends possessed physical properties, such as low lubricity, which were not compatible with conventional diesel fuel pumps. The fuel system eliminated the need for these liquid fuel blends to pass through conventional system.

A Horiba MEXA-9100HEGR automotive gas analyser system was used to measure the concentrations of CO, CO_2, THC, NO_x and O_2 in the engine exhaust gas. The analyser system housed a chemiluminescence analyser for NO_x (± 1 ppm), a flame ionization detector for THC (± 10 ppm), a non-dispersive infrared absorption analyser for CO (± 1 ppm) and CO_2 (± 0.01%), and a magneto-pneumatic analyser to measure oxygen (± 0.1%) concentrations. A differential mobility spectrometer from Cambustion (DMS500) was used to measure the exhaust particulate number and size distribution. Exhaust gas samples were collected 300 mm downstream of the exhaust valves and conveyed to the analysers via heated lines, which were maintained at 190 °C and 80 °C for the measurement of gaseous and particulate compositions, respectively.

3. Experimental methodology

3.1. Fuels investigated

Five alkylbenzenes – benzene, toluene, m-xylene, 1,3,5-trimethylbenzene and durene - were tested as binary mixtures with n-heptane so as to investigate the effect of varying the number of methyl branches on a monocyclic aromatic ring. In addition, benzaldehyde, which is an aromatic aldehyde consisting of a benzene ring with a formyl (-CHO) substituent, and which occurs as an intermediate during the oxidation reactions of alkylbenzenes, specifically toluene [31–33], was also tested. These six aromatic molecules were blended individually with n-heptane in different proportions (wt/wt) to form alkylbenzene/n-heptane binary blends, with n-heptane chosen as a single component fuel of ignition quality approximately equivalent to that of many fossil diesels. The authors were only able to test two blends of durene, 10% and 15%. The melting point of durene is 78 °C, and is therefore solid at room temperature. The authors were only able to dissolve up to 15% of durene in n-heptane. Adding any more durene resulted in solid durene settling at the bottom of the mixing flask, and not dissolving in the heptane.

A fossil diesel fuel was also tested as a reference fuel for all the experimental conditions investigated. Table 2 shows the molecular structure of each fuel tested, while Table 3 lists their assay and other physical properties.

Table 2
Molecular structures of fuels tested.

Benzene (BNZ)	
Toluene (TOL)	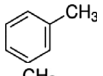
m-Xylene (M-XYL)	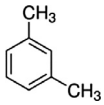
1,3,5-trimethylbenzene (1,3,5-TMB)	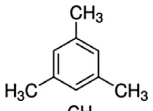
Durene (DUR)	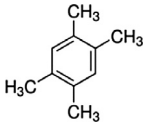
Benzaldehyde (BNZALDHYD)	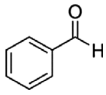
n-Heptane (HEP)	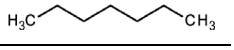

Table 3
Fuel properties (a - From supplier certificates/specification sheets, b - Initial boiling point, c - From European Chemicals Agency (ECHA) datasheets).

	Molecular formula	Assay (%)[a]	$T_{m.p}$ (°C)[a]	$T_{b.p}$ (°C)[a]	Density @20 °C (kg/m^3)[a]	Dynamic viscosity @25 °C (mPa.s)[c]	Cetane number [34]
BNZ	C_6H_6	99.8	5.5	80	877	0.604	–
TOL	$C_6H_5CH_3$	99.8	−93	110	866	0.560	4
M-XYL	$C_6H_4(CH_3)_2$	≥99	−48	139	860	0.581	10
1,3,5-TMB	$C_6H_3(CH_3)_3$	97	−45	165	861	0.727	−7
DUR	$C_6H_2(CH_3)_4$	98	78	–	838	–	6
BNZALDHYD	C_6H_5CHO	≥99.5	−26	179	1044	1.321	–
HEP	C_7H_{16}	99	−91	98	684	0.438	52
Fossil diesel	–	–	–	187.5[b]	826	–	52.7[a]

3.2. Test procedure

All the experiments in this study were conducted at an engine speed of 1200 rpm and at a fuel injection pressure of 450 bar. The engine was used in its naturally aspirated configuration, with no EGR or intake air boosting. The fuel injection duration was varied to keep the engine output load constant at 4 bar IMEP for all the tests.

Each of the binary blends and reference fossil diesel fuel were tested with two fuel injection timing approaches: constant start of fuel injection (SOI) and constant start of combustion ignition (SOC). SOI is defined as the time at which the actuation signal is sent to the fuel injector, while SOC is indicated by the first incidence of positive heat release after SOI and before the time of peak heat release rate. The duration of ignition delay is therefore defined as the time in crank angle degrees (CAD) between SOI and SOC. For the constant SOI tests, the fuel injection timing was fixed at 10 CAD BTDC and the start of combustion for each fuel varied according to its ignition delay. For the constant SOC, the fuel injection timing was varied so that the SOC of each fuel always occurred at piston TDC. Fig. 2 further demonstrates this by showing the heat release rate curves for both constant SOI and constant SOC tests. In some cases (as can be seen in Fig. 2), the binary fuel mixture showed a clear two stage combustion and, in these instances, the SOC was taken to be the time (in CAD) at which the second (or main) stage of combustion commenced.

4. Results and discussion

4.1. Combustion characteristics

Fig. 2 shows the apparent heat release rate curves for different m-xylene/n-heptane (M-XYL/HEP) binary mixtures and for reference diesel fuel, at a constant engine load of 4 bar IMEP, for both constant SOI and constant SOC timings. Similar graphs of heat release rate were plotted for the other alkylbenzenes, but have not been included in this paper to avoid repetition. Considering Fig. 2a, it can be observed that the ignition delay of the binary mixtures increases with increasing proportion of m-xylene in the mixture. Fig. 2a also shows that, up to a blend of 30% m-xylene in n-heptane, the binary mixtures undergo single stage combustion and the bulk of the heat release occurs during the premixed combustion, as indicated by the rapid increase of heat release rate following SOC. However, mixtures containing 45% or higher proportion of m-xylene undergo a distinctive two stage ignition type combustion. This two stage event is different from a typical compression ignition heat release, consisting of an initial much smaller heat release event, followed by the main heat release event as a result of a second ignition or combustion propagation. The interval between the two stages increases with the level of m-xylene in the mixture, with the bulk of heat release (for this mixture) occurring later in the expansion stroke. This results in comparatively slower rates of increase of heat release, lower peak heat release rates occurring further away from TDC and a more widespread premixed combustion stage (with a not so distinct diffusion-controlled burn stage). This can also be observed in Fig. 2b at constant SOC timings, where mixtures containing 45% or higher m-xylene have considerably lower peak heat release rates, as part of the fuel has already burned during the first stage of combustion. In comparison, fossil diesel fuel exhibits typical heat release with very distinctive premixed and diffusion-controlled burn stages (Fig. 2).

Fig. 3 shows the heat release rate curves for the different binary mixtures of aromatics in n−heptane, at a fixed proportion of 30% (wt/wt), for constant SOI at 10 CAD BTDC and fixed engine load of 4 bar IMEP. It can be observed from Fig. 3 that as the number of methyl branches on the aromatic molecule increases (going from benzene to 1,3,5-trimethylbenzene), the ignition delay increases and so does the timing at which peak heat release rate occurs, but the peak heat release rate remains largely similar. Further discussion on ignition delay and peak heat release rate, will be presented in the following paragraphs.

Fig. 4a and b show the duration of ignition delay for the different binary mixtures, and for n-heptane and reference diesel fuel for constant SOI and constant SOC timings and a fixed engine load of 4 bar IMEP. Considering Fig. 4a, it can be observed that as the proportion of the aromatic in the binary mixture is increased, the ignition delay increases, and this effect can be seen for all the mixtures. Furthermore,

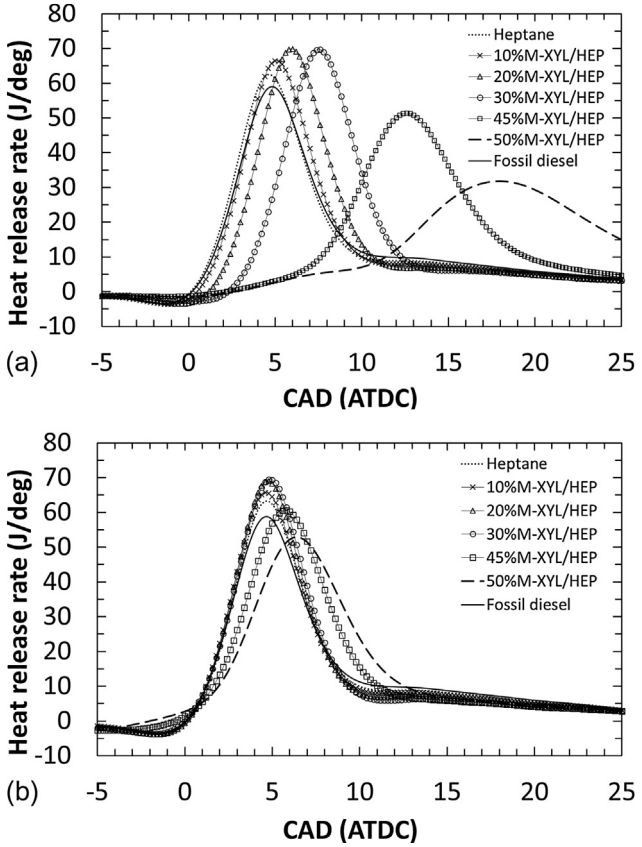

Fig. 2. Heat release rate curves of m-xylene/n-heptane binary mixtures for (a) constant start of fuel injection (SOI) at 10 CAD BTDC and (b) constant start of combustion (SOC) at TDC.

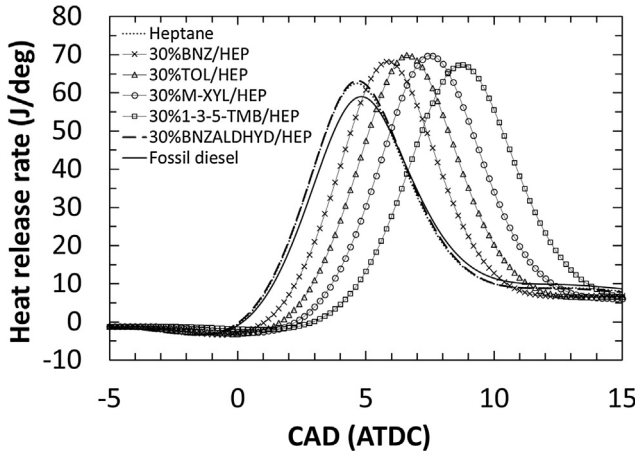

Fig. 3. Heat release rate curves of binary mixtures of various aromatics in n-heptane at a fixed proportion of 30% (wt/wt), for the constant SOI timing tests.

this increase in ignition delay is more pronounced for alkylbenzenes with a higher number for methyl branches. For example, considering a binary mixture of 45% of the alkylbenzene (Fig. 4a), the ignition delay is the shortest for benzene (with no methyl branch) and longest for 1,3,5-trimethylbenzene. The same trend of increasing ignition delay with increasing aromatic proportion can be seen in Fig. 4b when the combustion phasing is altered so that SOC occurs at engine TDC. Hence, it can be concluded that the ignition delay increases when the number of methyl branches in the binary mixture increases, whether that is by increasing the proportion of a given alkylbenzene in the binary mixture, or by having a alkylbenzene with a higher number of methyl branches.

The increase in ignition delay observed in Fig. 4 can be explained by considering the oxidation reaction pathway of toluene/n-heptane mixtures, which has been described in mechanistic studies in literature [31,33,35,36,22,37,38], and can also be applied to the other alkylbenzenes. The low temperature breakdown reactions of long chain alkanes such as n-heptane initiate with the formation of OH radicals, produced by abstraction of the H atom from n-heptane by O_2. This subsequently leads to the OH radicals abstracting further H atoms to breakdown the n-heptane into smaller molecules and form peroxy radicals and peroxides (such as H_2O_2) which, at compression temperatures, decompose and result in rapid branching reactions and propagate ignition [33,39]. However, in the presence of toluene, the OH radicals are also consumed to oxidise toluene to form benzyl radicals ($C_6H_5CH_2*$), whereby the H atom from the methyl branch of the toluene ring is substituted by the OH radical [31,35,36]. Benzyl radicals are thermally stable below 1000 K and cannot be further oxidised by O_2 [33,40]. Hence, it can be suggested that the methyl branch of an alkylbenzene molecule consumes the OH radicals that would otherwise be utilised in the radical propagating reactions of n-heptane leading to ignition. Therefore, the higher the proportion of alkylbenzenes in the binary mixtures or the higher the number of methyl branches on the aromatic rings, the more OH radicals would be consumed in stabilising benzyl radicals, reducing the pool of reactive radical species required for ignition and resulting in longer ignition delays. For example, it can be suggested that in the case of m-xylene, twice as many OH radicals per alkylbenzene molecule may be removed from the radical pool, as compared to toluene.

Another possible reason for the increase in ignition delay could be the presence of the relatively non-reactive alkylbenzenes diluting the in-cylinder mixture and reducing the access to O_2, and thereby, rates of reaction of the comparatively more reactive n-heptane. For example, it is known that toluene does not exhibit significant low temperature reactivity that would result in heat release [41]. Furthermore, the physical properties of the alkylbenzenes could also be a factor in increasing the ignition delay. All the alkylbenzenes tested in this work have higher boiling points, densities, and dynamics viscosities as compared to n-heptane (Table 3), which is likely to have reduced the efficiency of the fuel and air mixing during the ignition delay period.

In the case of benzene (Fig. 4a), the low temperature fuel breakdown reactions involve the abstraction of an H atom from the benzene ring by O_2 and other radicals (OH, H, O) to form phenyl radicals. Unlike the benzyl radical which is stable below 1000 K, the phenyl radical can undergo further oxidation and ring fragmentation reactions, which subsequently leads to the liberation of considerable thermal energy [31,38,42–44]. The absence of any methyl branches on the aromatic ring and the relative reactivity of the phenyl radical could therefore most likely explain the shorter ignition delays of benzene binary mixtures as compared to those for the other alkylbenzenes (Fig. 4a). However, as the proportion of benzene in the binary mixture increases, the ignition delay increases since benzene consumes the radical species that could otherwise be used for the branching reactions.

Another interesting observation in Fig. 4a and b concerning the benzaldehyde/n-heptane mixtures has been outlined in this paragraph. When the proportion of benzaldehyde in the binary mixture is increased up to 10%, the ignition delay reduces by 1 CAD, however, above this level of benzaldehyde addition an increase in ignition delay is observed. (Note that these tests were repeated several times to make sure that the reduction in ignition delay was real and not a random experimental anomaly). A likely explanation for the initial reduction could be that benzaldehyde readily breaks down yielding phenyl (C_6H_5) and formyl (CHO) radicals [31,33]. Formyl radicals have been identified as being key intermediates in the active chain branching sequence of formaldehyde oxidation. In oxidising environments, formyl radicals rapidly decompose to yield CO and H – the H radical then reacts with formaldehyde to produce more formyl radicals [42].It is possible that the presence of the formyl radical initially accelerates the low

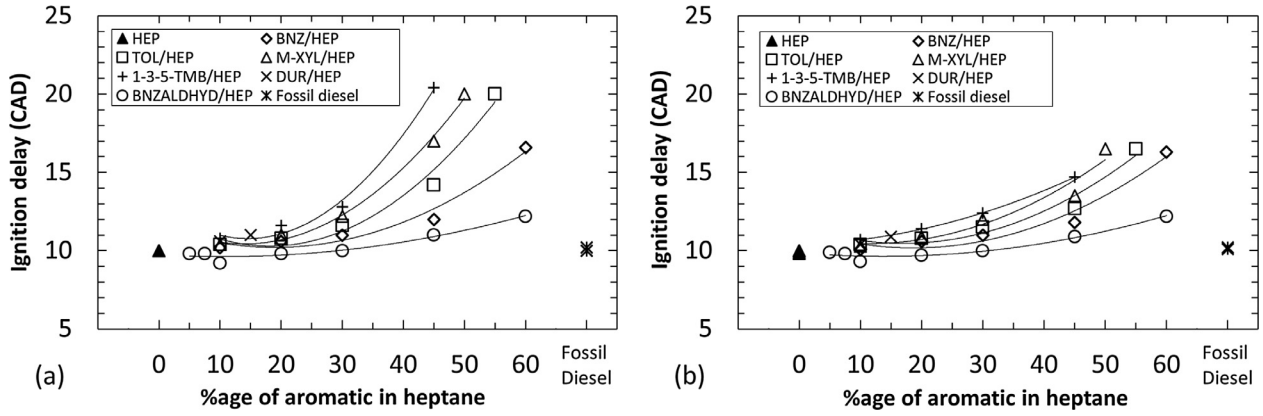

Fig. 4. Duration of ignition delay for the different binary mixtures, at a constant load of 4 bar IMEP, for (a) constant SOI and (b) constant SOC timings.

temperature breakdown reactions, hence reducing the ignition delay. However, as discussed earlier, the phenyl radicals act as sinks to consume reactive radicals, thus increasing ignition delay. As the proportion of benzaldehyde in the binary mixture is increased, the effect of phenyl radicals, combined with their considerably higher boiling points, densities and viscosities (compared to n-heptane, Table 3). It should be noted that benzaldehyde, despite having a considerably higher boiling point, density and viscosity of as compared to the rest of the alkylbenzenes, exhibited the shortest ignition delays of all the binary mixtures, most probably due to formation of the highly reactive formyl radicals.

Fig. 5 shows the peak heat release rates (pHRR) and the time of peak heat release rates (tPHRR) for the various binary mixtures, and for n-heptane and reference diesel fuel, at a constant engine load of 4 bar IMEP. Considering Fig. 5a, it can be observed that as the proportion of each alkylbenzene is increased in the binary mixture, the peak heat release rates initially increase slightly and subsequently decrease significantly. This can be explained in the context of the ignition delay (Fig. 4a) and tPHRR (Fig. 5c) results. For mixtures containing up to 30% of the alkylbenzene, the ignition delay shows an appreciable increase with increasing percentage of alkylbenzene. This allows more time for the fuel and air to mix, and a greater amount of premixed fraction available for ignition at SOC. At the same time, this ignition delay period is not long enough for the tPHRR to occur too far into the expansion stroke. For mixtures containing up to 30% of the alkylbenzene, the tPHRR only extends up to 8 CAD ATDC, with the piston still quite near its TDC position. Therefore, the increased ignition delay combined with heat release occurring close to TDC, results in higher peak heat release rates as the proportion of alkylbenzene in the mixture increases. However, a further increase in ignition delay would result in the heat release to occur increasingly further into the expansion stroke, causing a greater surface area of the cylinder wall to be exposed to the hot combustion gases, leading to higher rates of heat transfer from cylinder gases. Therefore, beyond 30% aromatic content, the ignition delay increases considerably (Fig. 4a) and heat release occurs quite far into the expansion stroke (Fig. 5c), resulting in much lower peak heat release rates, as can be seen in Fig. 5a. Additionally, in some cases when the proportion of the alkylbenzene is quite high (40% or more), the binary mixture undergoes two-stage combustion. This could be because, as discussed earlier, the alkylbenzenes in the mixture act as sinks to remove OH radicals during the ignition delay period, preventing the build-up of sufficient radicals to initiate ignition throughout the cylinder charge. Only a portion of the charge reacts during the first stage, and additional time is required for more fuel and air to mix to near-stoichiometric conditions for combustion in the second stage. It is also likely that local gas temperatures are higher due to the first stage of heat release, which also helps in propagating ignition throughout the remaining cylinder charge during the second stage. A consequence of two-stage ignition is that the bulk of heat release occurs far into the expansion stroke, resulting in low peak heat release rates, as can be observed in the heat release trace for 50% m-xylene/n-heptane mixtures in Fig. 2a. Considering Fig. 5b and d, the trends in pHRR and tPHRR are similar for the constant SOC timing, though the reduction in pHRR is not as pronounced since ignition occurs at TDC, and therefore the heat release occurs relatively early in the expansion stroke for all the mixtures.

Fig. 5a also shows the drop in pHRR when the proportion of benzaldehyde in the mixture is increased up to 10%. This agrees with the results for benzaldehyde ignition delay discussed earlier (Fig. 4a), and is attributable to the reduction in ignition delay resulting in less time for fuel and air to mix, and hence lower peak heat release rates. As the percentage of benzaldehyde is increased, the ignition delay increases and so do the peak heat release rates, before eventually decreasing (above 50% benzaldehyde in the mixture) as the heat release occurs further into the expansion stroke.

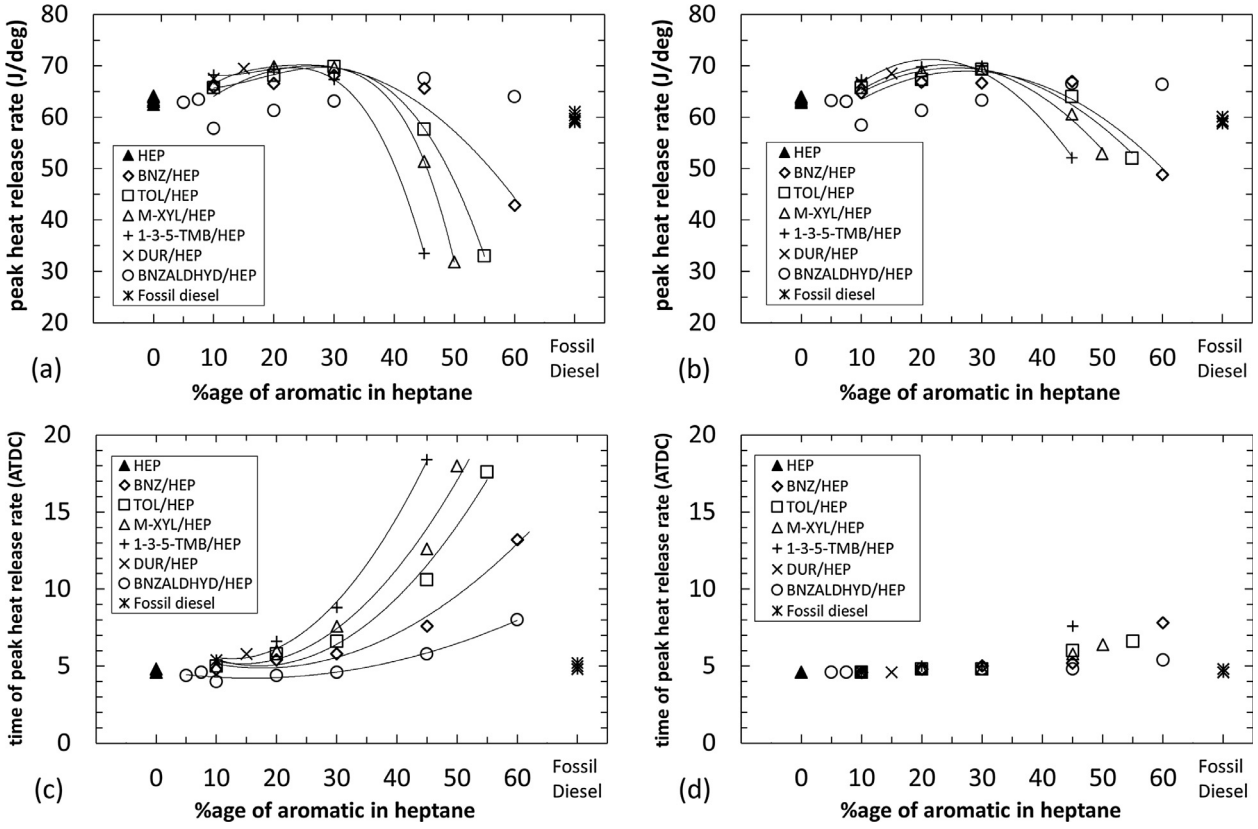

Fig. 5. Combustion characteristics for the different binary mixtures at 4 bar IMEP for constant SOI and constant SOC timings: (a) and (b) peak heat release rates; (c) and (d) time of peak heat release rates.

4.2. CO_2, CO and unburned THC exhaust gas emissions

Fig. 6a and b shows the CO_2 exhaust emissions for the different binary mixtures, and for n-heptane and reference diesel fuel, for constant SOI and constant SOC timings and a fixed engine load of 4 bar IMEP. The CO_2 emissions are quite similar for the various binary mixtures, with the highest CO_2 emissions shown by the benzaldehyde mixtures. For some of the alkylbenzene mixtures, such as toluene or m-xylene, a small reduction in CO_2 emissions is observed when the proportion of the alkylbenzene is increased above 30%. This could be attributed to the bulk of the heat release occurring very late into the expansion stroke, resulting in reduced rates of oxidation reactions, and lower CO_2 emissions.

Fig. 6c and e show, respectively, the CO and unburned THC exhaust emissions for the different binary mixtures, at a fixed engine load of 4 bar IMEP, for the constant SOI timing. It can be observed, in the case of both the CO and THC emissions, that below 30% alkylbenzene blend levels, the change in the emission levels is not significant. However, above the 30% level, the CO and THC emissions increase very rapidly. This sharp increase could be attributed to the long ignition delay periods and reduced peak heat release rates occurring further into the expansion stroke, resulting in lower in-cylinder gas temperatures and reduced rates of oxidation reactions, and hence higher emissions of CO and THC. Another potential reason for the high emissions of CO and THC could be that some fuel mixes with air beyond the lean combustion limit due to long ignition delay periods caused by high blend proportions of alkylbenzenes, as observed in Fig. 4a. This over-dilution of the fuel prevents the mixture from autoigniting or being able to sustain a fast flame front, hence resulting in unburned fuel, and the formation of partial fuel oxidation and fuel decomposition products [45,46].

Interestingly, considering Fig. 6, the reduction in CO_2 emissions is related to CO emissions. For example, in Fig. 6b and d, at 45% aromatic content in heptane, benzaldehyde shows the lowest CO emissions but the highest CO_2 emissions. Similarly, 1,3,5-trimethylbenzene shows the

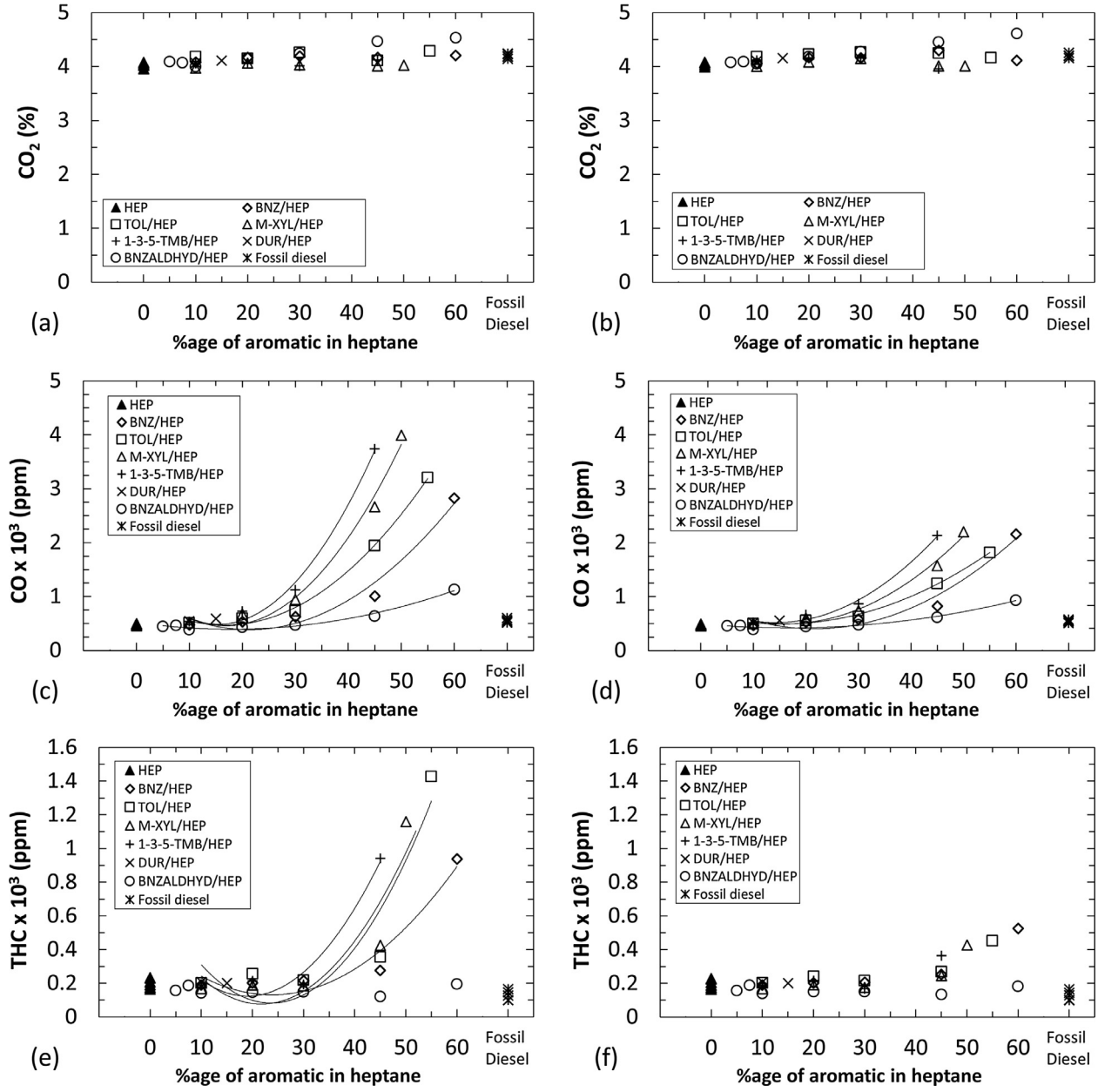

Fig. 6. Variation in the exhaust emissions of (a) and (b) carbon dioxide (CO_2), (c) and (d) carbon monoxide (CO), and (e) and (f) unburned total hydrocarbons (THC) for constant SOI and constant SOC timings, for the different binary mixtures.

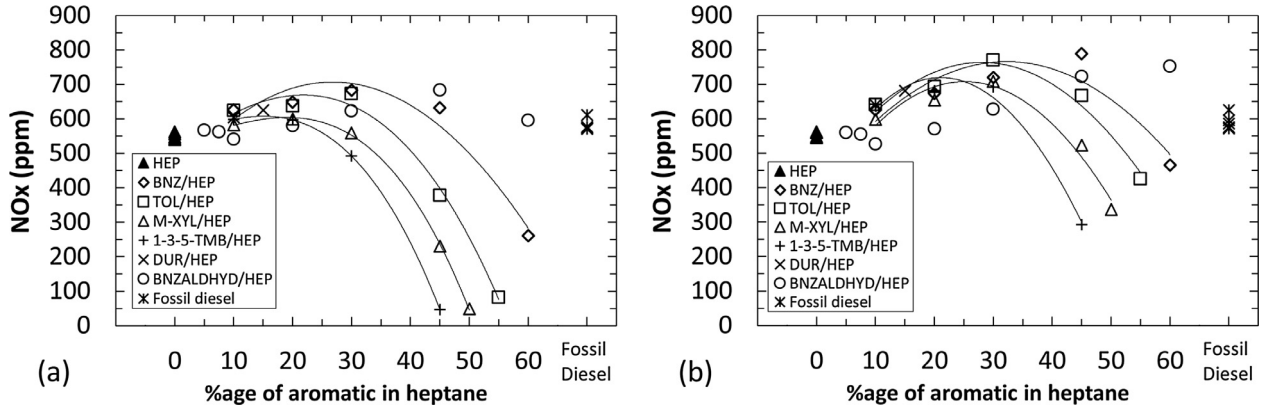

Fig. 7. Variation in the exhaust emissions of oxides of nitrogen (NO_x), for constant SOI and constant SOC timings, for the different binary mixtures.

highest CO emissions, but the lowest CO_2 emissions. Hence, the benzaldehyde has a higher combustion efficiency resulting in higher CO_2 emissions.

4.3. NO_x exhaust gas emissions

Fig. 7 shows the NO_x exhaust emissions for the different binary mixtures, and for n-heptane and reference diesel fuel, for constant SOI and constant SOC timings and a fixed engine load of 4 bar IMEP. Considering Fig. 7a, it can be observed that as the proportion of the alkylbenzenes in the binary mixtures increases, the NO_x emissions initially increase and then subsequently decrease substantially. This trend agrees with the peak heat release rates (Fig. 5a), which is expected since heat release rates are an indication of the in-cylinder gas temperatures. It is known that the rate of NO_x formation is highly thermally sensitive [47,48], and NO_x production primarily takes place in the post flame gases following the premixed burn stage, predominantly due to the high gas temperatures present under such conditions [46,49]. As the proportion of alkylbenzenes is increased up to 30% in the mixtures, the increase in ignition delay (Fig. 4a), combined with the bulk of heat release continuing to occur relatively close to TDC (Fig. 5c), results in in-cylinder temperatures high enough to accelerate NO_x formation rates. However, beyond 30% alkylbenzene content, the bulk of heat release occurs further intro the expansion stroke, where the heat losses to the cylinder walls are considerable and the in-cylinder gas temperatures do not reach the threshold for significant NO_x formation, leading to a sharp fall in exhaust NO_x emissions, as observed in Fig. 7a.

For the constant SOC tests (Fig. 7b), the NO_x emissions exhibit similar trends, however, the absolute values of NO_x emissions are higher than those for the constant SOI tests, since the heat release occurs closer to TDC, resulting in relatively higher gas temperatures and longer residence times are these temperatures. The trend in NO_x emissions for the benzaldehyde binary mixtures in both Fig. 7a and b is concurs with the ignition delay and peak heat release rate trends observed in Figs. 4a and 5a respectively, the reasons for which have been discussed in detail earlier in Section 4.1.

4.4. Particulate exhaust emissions

Fig. 8 shows the exhaust particulate mass (TPM) emissions for the different binary mixtures, and for n-heptane and reference diesel fuel, for constant SOI and constant SOC timings and a fixed engine load of 4 bar IMEP. As the proportion of the alkylbenzenes is increased in the binary mixtures, no definitive trend is evident in the TPM emissions. However, TPM emissions from 1,3,5-trimethylbenzene/n-heptane mixtures are distinctively high as compared to other alkylbenzenes, for both the constant SOI and constant SOC tests. The high TPM emissions could be attributed to the 1,3,5-trimethylbenzene having the highest viscosity and boiling point of all the alkylbenzenes tested in this study (Table 3). This could lead to a reduction in the efficiency of the in-cylinder fuel and air mixing process, resulting in fuel-rich pockets inside the combustion chamber which are could be expected to form particulates. The lower TPM emission of durene, as compared to 1,3,5 TMB, is probably due to the higher cetane number of durene (6) as compared to TMB (-7), as outlined in Table 3, therefore making durene easier to ignite.

Fig. 9 shows the size distribution of the number of particulates in the engine exhaust for the different binary mixtures, all with 30%

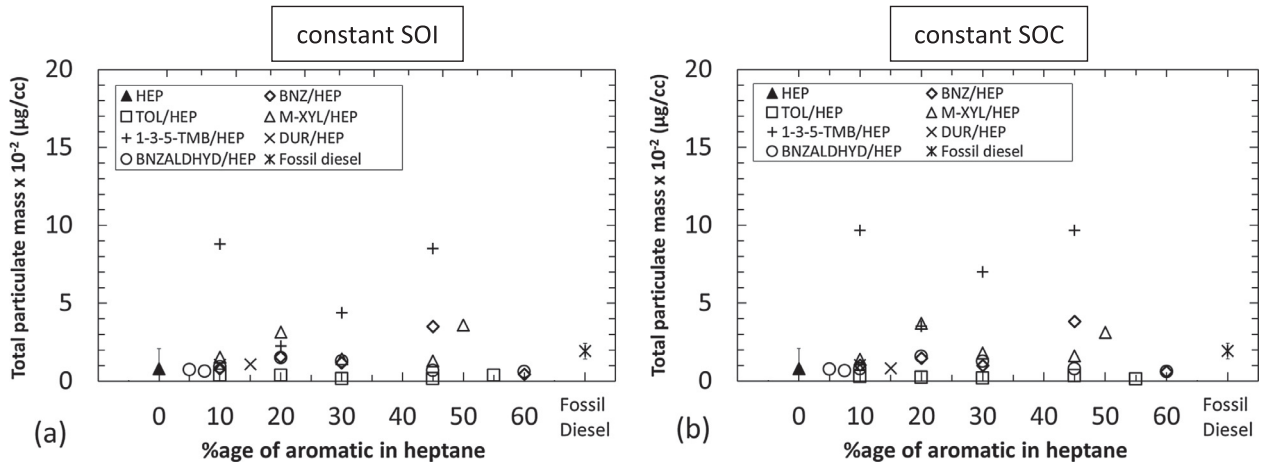

Fig. 8. Variation in the exhaust emissions of total particulate mass, for the different binary mixtures, at constant SOI and constant SOC timings.

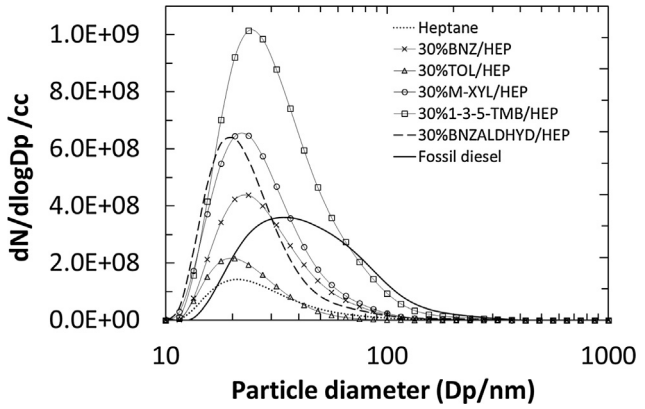

Fig. 9. Particulate number distribution at a constant engine load of 4 bar IMEP for binary mixtures with 30% blend of the different aromatics in n-heptane.

aromatic content. For comparison, the size distribution for n-heptane and reference fossil diesel is also shown. The lowest number of particles with the smallest range of diameters is from n-heptane which could be expected, as it has no aromatic content – aromatics are known precursors of particulates [50]. In agreement with the total particulate mass results (Fig. 8), the 1,3,5-trimethylbenzene/n-heptane mixtures produced, by a significant amount, the highest number of particles covering the widest range of particle diameters, as compared to the other binary mixtures tested (Fig. 9). As discussed earlier, this could be attributable to the comparatively higher viscosity and boiling point of 1,3,5-trimethylbenzene. It can also be observed from Fig. 9 that increasing the number of methyl groups on the aromatic ring tends to increase the number of particles formed, with the exception of toluene, which formed the lowest number of particles of all the alkylbenzene binary mixtures. The increase in the number of particles with increasing number of methyl branches agrees with the conclusions presented in a recent study [51] which investigated the sooting propensity of different alkylbenzenes using a variety of microscopic and spectroscopic techniques. The higher sooting tendencies of alkylbenzenes with a larger number of methyl branches are suggested to be attributable to the formation of resonant stabilized radicals (RSRs), such as benzyl, as compared to benzene which forms phenyl radicals [44]. The RSRs can survive for longer in high temperature flame environments relative to phenyl radicals, and therefore, are more likely to form particulates [52,53].

5. Conclusions

1. The ignition delay increased with increasing number of methyl branches on the aromatic ring, due to the alkylbenzenes consuming the highly reactive OH radicals required for the escalation of ignition.
2. For up to 10% benzaldehyde content in the binary mixture, the ignition delay decreased, which was attributed to the formation of formyl (CHO) radicals. These radicals readily decompose and accelerate the rapid branching reactions which lead to ignition.
3. Peak heat release rates initially increased due to increased duration of ignition delay, but subsequently decreased because of substantially longer ignition delay periods, resulting in the bulk of heat release occurring late in the expansion stroke and promoting greater thermal losses from the combustion gases to the engine cylinder wall.
4. Above 30% alkylbenzene content in the binary mixture, exhaust CO and unburned THC emissions increased rapidly due to reduced rates of oxidation reactions, as a result of lower peak heat release rates and overleaning of some of the in-cylinder fuel-air mixture.
5. Exhaust NO_x emissions were primarily driven by ignition delay and peak heat release rates, and decreased quite sharply when post-combustion in-cylinder gas temperatures dropped due to low peak heat release rates.
6. The number of particles produced by the binary mixtures increased with increasing number of methyl branches on the aromatic ring (with the exception of toluene). This was attributed to the alkylbenzenes with methyl branches forming thermally stable benzyl radicals, as compared to benzene which forms phenyl radicals and undergo oxidation relatively readily.

It can be seen from the results that the effect of increasing the number of methyl branches on an aromatic ring is, to a large extent, similar to increasing the proportion of an alkylbenzene in the fuel blend. That is, the effect on combustion characteristics and emissions is observed to be primarily dependent on the concentration of methyl branches in the fuel. The results also show that the addition of up to 30% alkylbenzene content in heptane does not significantly increase the ignition delay, thereby having no significant effect on the combustion phasing. However, for blends containing higher than 30% alkylbenzene content, the ignition delay increases considerably, resulting in a two-stage ignition type combustion event with the main bulk of heat release occurring well into the expansion stroke, and leading to higher emissions of partially oxidised combustion products such as CO and unburned THCs.

Acknowledgements

The authors would also like to acknowledge EPRSC (EP/M009424/1 and EP/M007960/1) for their support to this project.

References

[1] Unfccc. Kyoto Protocol. United Nations Framew Conv Clim Chang 1998;2011:795–811. doi:10.2968/064001011.
[2] United Nations/Framework Convention on Climate Change. Paris Agreement. 21st Conf Parties 2015:3. doi:FCCC/CP/2015/L.9.
[3] European Commission, European Parliament and Council. Directive 2009/28/EC of the European Parliament and of the Council of 23 April 2009 on the promotion of the use of energy from renewable sources and amending and subsequently repealing Directives 2001/77/EC and 2003/30/EC (Text with EEA relevance). Off J Eur Union 2009:16–62.
[4] US EPA. Renewable Fuel Standard (RFS). Fuels Fuel Addit 2005.
[5] Yang H, Zhou Y, Liu J. Land and water requirements of biofuel and implications for food supply and the environment in China. Energy Policy 2009;37:1876–85. http://dx.doi.org/10.1016/j.enpol.2009.01.035.
[6] Röder M. More than food or fuel. Stakeholder perceptions of anaerobic digestion and land use; a case study from the United Kingdom. Energy Policy 2016;97:73–81. http://dx.doi.org/10.1016/j.enpol.2016.07.003.
[7] Man Y, Xiao H, Cai W, Yang S. Multi-scale sustainability assessments for biomass-based and coal-based fuels in China. Sci Total Environ 2017;599–600:863–72. http://dx.doi.org/10.1016/j.scitotenv.2017.05.006.
[8] Carneiro MLNM, Pradelle F, Braga SL, Gomes MSP, Martins ARFA, Turkovics F, et al. Potential of biofuels from algae: comparison with fossil fuels, ethanol and biodiesel in Europe and Brazil through life cycle assessment (LCA). Renew Sustain Energy Rev 2017;73:632–53. http://dx.doi.org/10.1016/j.rser.2017.01.152.
[9] Wu Y, Zhang S, Hao J, Liu H, Wu X, Hu J, et al. On-road vehicle emissions and their control in China: a review and outlook. Sci Total Environ 2017;574:332–49. http://dx.doi.org/10.1016/j.scitotenv.2016.09.040.
[10] Thiel C, Schmidt J, Van Zyl A, Schmid E. Cost and well-to-wheel implications of the vehicle fleet CO2 emission regulation in the European Union. Transp Res Part A Policy Pract 2014;63:25–42. http://dx.doi.org/10.1016/j.tra.2014.02.018.
[11] Boot MD, Tian M, Hensen EJM, Mani Sarathy S. Impact of fuel molecular structure on auto-ignition behavior – design rules for future high performance gasolines. Prog Energy Combust Sci 2017;60:1–25. http://dx.doi.org/10.1016/j.pecs.2016.12.001.
[12] Heywood JB. Internal Combustion Engine Fundamentals vol. 21. Internatio: McGraw-Hill Book Company; 1988.
[13] Hellier P, Ladommatos N, Allan R, Rogerson J. The influence of fatty acid ester alcohol moiety molecular structure on diesel combustion and emissions. Energy and Fuels 2012;26:1912–27. http://dx.doi.org/10.1021/ef2017545.
[14] Tuck CO, Pérez E, Horváth IT, Sheldon RA, Poliakoff M. Valorization of Biomass: Deriving More Value from Waste. Science (80-) 2012;337.
[15] Dautzenberg G, Gerhardt M, Kamm B. Bio based fuels and fuel additives from lignocellulose feedstock via the production of levulinic acid and furfural. Holzforschung 2011;65:439–51. http://dx.doi.org/10.1515/hf.2011.081.
[16] Alonso DM, Wettstein SG, Dumesic JA. Bimetallic catalysts for upgrading of biomass to fuels and chemicals. Chem Soc Rev 2012;41:8075. doi:10.1039/c2cs35188a.

[17] Huber GW, Iborra S, Corma A. Synthesis of transportation fuels from biomass: chemistry, catalysts, and engineering. Chem Rev 2006;106:4044–98.
[18] Thring RW, Katikaneni SPR, Bakhshi NN. The production of gasoline range hydrocarbons from Alcell□ lignin using HZSM-5 catalyst. Fuel Process Technol 2000;62:17–30.
[19] Zhang Y, Bi P, Wang J, Jiang P, Wu X, Xue H, et al. Production of jet and diesel biofuels from renewable lignocellulosic biomass. Appl Energy 2015;150:128–37. http://dx.doi.org/10.1016/j.apenergy.2015.04.023.
[20] Yan WH, Duan PG, Wang F, Xu YP. Composition of the bio-oil from the hydrothermal liquefaction of duckweed and the influence of the extraction solvents. Fuel 2016;185:229–35. http://dx.doi.org/10.1016/j.fuel.2016.07.117.
[21] Yanowitz J, Ratcliff MA, Mccormick RL, Tay JD, Murphy MJ. Compendium of Experimental Cetane Numbers. 2014.
[22] Hellier P, Ladommatos N, Allan R, Rogerson J. Combustion and emissions characteristics of toluene/n-heptane and 1-octene/n-octane binary mixtures in a direct injection compression ignition engine. Combust Flame 2013;160:2141–58. http://dx.doi.org/10.1016/j.combustflame.2013.04.016.
[23] Baumgardner ME, Vaughn TL, Lakshminarayanan A, Olsen D, Ratcliff MA, McCormick RL, et al. Combustion of lignocellulosic biomass based oxygenated components in a compression ignition engine. Energy & Fuels 2015;29:7317–26. http://dx.doi.org/10.1021/acs.energyfuels.5b01595.
[24] Ladommatos N, Rubenstein P, Bennett P. Some effects of molecular structure of single hydrocarbons on sooting tendency. Fuel 1996;75:114–24.
[25] Mensch A, Santoro RJ, Litzinger TA, Lee SY. Sooting characteristics of surrogates for jet fuels. Combust Flame 2010;157:1097–105. doi:https://doi.org/10.1016/j.combustflame.2010.02.008.
[26] Calcote HF, Manos DM. Effect of molecular structure on incipient soot formation. Combust Flame 1983;49:289–304. http://dx.doi.org/10.1016/0010-2180(83)90172-4.
[27] Talibi M, Balachandran R, Ladommatos N. Influence of combusting methane-hydrogen mixtures on compression–ignition engine exhaust emissions and in-cylinder gas composition. Int J Hydrogen Energy 2017;42:2381–96. http://dx.doi.org/10.1016/j.ijhydene.2016.10.049.
[28] Schönborn A, Ladommatos N, Williams J, Allan R, Rogerson J. Effects on diesel combustion of the molecular structure of potential synthetic bio-fuel molecules. SAE 2007. http://dx.doi.org/10.4271/2007-24-0125.
[29] Hellier P, Ladommatos N, Allan R, Payne M, Rogerson J. The Impact of Saturated and Unsaturated Fuel Molecules on Diesel Combustion and Exhaust Emissions. SAE Pap 2011:2011–01–1922. doi:10.4271/2011-01-1922.
[30] Talibi M. Co-combustion of diesel and gaseous fuels with exhaust emissions analysis and in-cylinder gas sampling. PhD Thesis (Doctoral), University College London, 2015.
[31] Simmie JM. Detailed chemical kinetic models for the combustion of hydrocarbon fuels. Prog Energy Combust Sci 2003;29:599–634. http://dx.doi.org/10.1016/S0360-1285(03)00060-1.
[32] Brezinsky K, Litzinger TA, Glassman I. The high temperature oxidation of the methyl side chain of toluene. Int J Chem Kinet 1984;16:1053–74. http://dx.doi.org/10.1002/kin.550160902.
[33] Emdee JL, Brezinsky K, Glassman I. A kinetic model for the oxidation of toluene near 1200 K. J Phys Chem 1992;96:2151–61. http://dx.doi.org/10.1021/j100184a025.
[34] Do PTM, Crossley S, Santikunaporn M, Resasco DE. Catalytic strategies for improving specific fuel properties. Catalysis, Cambridge: Royal Society of Chemistry; n.d., p. 33–64. doi:10.1039/b602366p.
[35] Andrae J, Johansson D, Björnbom P, Risberg P, Kalghatgi G. Co-oxidation in the auto-ignition of primary reference fuels and n-heptane/toluene blends. Combust Flame 2005;140:267–86. http://dx.doi.org/10.1016/j.combustflame.2004.11.009.
[36] Vanhove G, Petit G, Minetti R. Experimental study of the kinetic interactions in the low-temperature autoignition of hydrocarbon binary mixtures and a surrogate fuel. Combust Flame 2006;145:521–32. http://dx.doi.org/10.1016/j.combustflame.2006.01.001.
[37] Lindstedt RP, Maurice LQ. Detailed kinetic modelling of toluene combustion. Combust Sci Technol 1996;120:119–67. http://dx.doi.org/10.1080/00102209608935571.
[38] Davis SG, Law CK. Determination of and fuel structure effects on laminar flame speeds of C 1 to C 8 hydrocarbons. Combust Sci Technol 1998;140:427–49. http://dx.doi.org/10.1080/00102209808915781.
[39] Westbrook CK. Chemical kinetics of hydrocarbon ignition in practical combustion systems. Proc Combust Inst 2000;28:1563–77. http://dx.doi.org/10.1016/S0082-0784(00)80554-8.
[40] Griffiths JF, Mohamed C. Spontaneous ignition delays as a diagnostic of the propensity of aikanes to cause engine knock n.d.; 2180:4–7.
[41] Griffiths JF, Halford-Maw PA, Rose DJ. Fundamental features of hydrocarbon autoignition in a rapid compression machine. Combust Flame 1993;95:291–306. http://dx.doi.org/10.1016/0010-2180(93)90133-N.
[42] Westbrook CK, Dryer FL. Chemical kinetic modeling of hydrocarbon combustion. Prog Energy Combust Sci 1984;10:1–57. http://dx.doi.org/10.1016/0360-1285(84)90118-7.
[43] Norrish RGW, Taylor GW. The oxidation of benzene. Proc R Soc A Math Phys Eng Sci 1956;234:160–77. http://dx.doi.org/10.1098/rspa.1956.0024.
[44] Li Y, Zhang L, Yuan T, Zhang K, Yang J, Yang B, et al. Investigation on fuel-rich premixed flames of monocyclic aromatic hydrocarbons: part I. Intermediate identification and mass spectrometric analysis. Combust Flame 2010;157:143–54. http://dx.doi.org/10.1016/j.combustflame.2009.07.021.
[45] Greeves G, Khan IM, Wang CHT, Fenne I. Origins of hydrocarbon emissions from diesel engines. SAE Trans 770259 1977;86. doi:10.4271/770259.
[46] Heywood JB. Internal Combustion Engine Fundamentals. 1st ed. New York: McGraw-Hill; 1988.
[47] Miller JA, Bowman CTC. Mechanism and modeling of nitrogen chemistry in combustion. Prog Energy Combust Sci 1989;15:287–338. http://dx.doi.org/10.1016/0360-1285(89)90017-8.
[48] Bowman CT. Kinetics of nitric oxide formation incombustion processes. Symp Combust 1973;14:729–38. http://dx.doi.org/10.1016/S0082-0784(73)80068-2.
[49] Turns SR. An Introduction to Combustion: Concepts and Applications. New York: McGraw-Hill; 1996.
[50] Tree DR, Svensson KI. Soot processes in compression ignition engines. Prog Energy Combust Sci 2007;33:272–309. http://dx.doi.org/10.1016/j.pecs.2006.03.002.
[51] Guerrero Peña GDJ, Alrefaai MM, Yang SY, Raj A, Brito JL, Stephen S, et al. Effects of methyl group on aromatic hydrocarbons on the nanostructures and oxidative reactivity of combustion-generated soot. Combust Flame 2016;172:1–12. http://dx.doi.org/10.1016/j.combustflame.2016.06.026.
[52] Violi A, Sarofim A, Truong T. Quantum mechanical study of molecular weight growth process by combination of aromatic molecules. Combust Flame 2001;126:1506–15. http://dx.doi.org/10.1016/S0010-2180(01)00268-1.
[53] Sinha S, Raj A. Polycyclic aromatic hydrocarbon (PAH) formation from benzyl radicals: a reaction kinetics study. Phys Chem Chem Phys 2016;18:8120–31. http://dx.doi.org/10.1039/C5CP06465A.